applied sciences

MDPI

Article

Limonin Derivatives via Hydrogenation: Structural Identification and Anti-Inflammatory Activity Evaluation

Jingguo Yang [1], Yuhong Hu [1,2] and Kuan Chang [1,*]

[1] Key Laboratory of Synthetic and Biological Colloids, Ministry of Education, School of Chemical and Material Engineering, Jiangnan University, Wuxi 214122, China
[2] Quzhou Zhanhong Biotechnology Co., Ltd., Quzhou 324000, China
* Correspondence: changkuan@jiangnan.edu.cn

Abstract: Limonin is a natural compound which is rich in the fruit of various plants of the Rutaceae family and demonstrated to have a wide range of biological activities. In this work, seven limonin derivatives were successfully synthesized by hydrogenation of limonin, using different reducing agents (sodium cyanoborohydride, lithium aluminum hydride, and sodium borohydride). The chemical structure of the seven derivatives was characterized and identified by a series of techniques, including HR-ESI-MS, 1H-NMR, 13C-NMR, 2D-NMR, and IR. Among the seven limonin derivatives, six limonin derivatives were found to be new compounds which have not been previously reported. Then, the anti-inflammatory activities of the seven synthesized limonin derivatives, as well as the anti-inflammatory activities of eight known natural limonins, were evaluated and compared. Natural limonins, 30-*O*-Acetylhainangranatumin E and Xylogranatin A, presented significantly better anti-inflammatory activity. Xylogranatin A could inhibit LPS-induced RAW264.7 cell inflammatory factors, with a 90.0% inhibition ratio of TNF-α and 63.77% inhibition ratio of NO release in LPS-induced BV2 cells at 10 μM. Other natural limonins showed poor anti-inflammatory activity. In comparison, all the synthetic limonin derivatives showed decent anti-inflammatory activities, with the highest inhibition ratio of TNF-α of 37.8% and inhibition ratio of NO release of 12.5% in LPS-induced BV2 cells at 10 μM.

Keywords: limonins; structural modification; biological activity; anti-inflammatory

check for updates

Citation: Yang, J.; Hu, Y.; Chang, K. Limonin Derivatives via Hydrogenation: Structural Identification and Anti-Inflammatory Activity Evaluation. *Appl. Sci.* **2022**, *12*, 11169. https://doi.org/10.3390/app122111169

Academic Editor: Catarina Guerreiro Pereira

Received: 16 October 2022
Accepted: 28 October 2022
Published: 4 November 2022

Publisher's Note: MDPI stays neutral with regard to jurisdictional claims in published maps and institutional affiliations.

Copyright: © 2022 by the authors. Licensee MDPI, Basel, Switzerland. This article is an open access article distributed under the terms and conditions of the Creative Commons Attribution (CC BY) license (https://creativecommons.org/licenses/by/4.0/).

1. Introduction

Limonoids are a class of natural compounds in plants, mainly found in the tissues of Meliaceae and Rutaceae plants. They are the most abundant among the plants in the Rutaceae family, especially in the fruits and seeds of citrus, such as pomelo, sweet orange, and lemon [1]. More than 130 natural limonoid compounds have been isolated and identified from plants belonging to the Meliaceae and Rutaceae families [2–4]. The structures of some compounds are illustrated in Figure 1.

In recent years, intensive developments have been made in biopharmacological studies on limonin [5]. Studies have shown that limonin has excellent anti-inflammatory properties [4]. It can efficiently regulate the inflammatory response mediated by $CD4^+$ T cells and inhibit the proliferation of $CD4^+$ T cells by hindering the nuclear translocation of Nuclear Factor κB (NF-κB) in activated $CD4^+$ T cells [6]. Moreover, limonin participates in the regulation of inflammatory pathways by effectively inhibiting the activity of p38 mitogen-activated protein (MAP) kinase in vascular smooth muscle cells [7]. Through attenuating inflammation and fibrosis, it can also offset hypertension and vascular damage associated with metabolic syndrome (MetS) [8]. Moreover, limonin can effectively inhibit excessive nitric oxide (NO) production which is induced by the lipopolysaccharide (LPS), in RAW264.7 mouse macrophage cells, with an IC_{50} (half maximal inhibitory concentration) of 231.4 μM. The mechanism whereby this occurs is that the expression of the iNOS gene is inhibited

by the NF-κB mediated pathway, thus hampering NO production [9]. In addition, many studies have shown that limonin also has excellent antitumor, antibacterial, and antiviral activities [10–16]. As a pure plant-based substance, limonin has vast application potential in developing functional raw materials for products like cosmetics, food, and medicine.

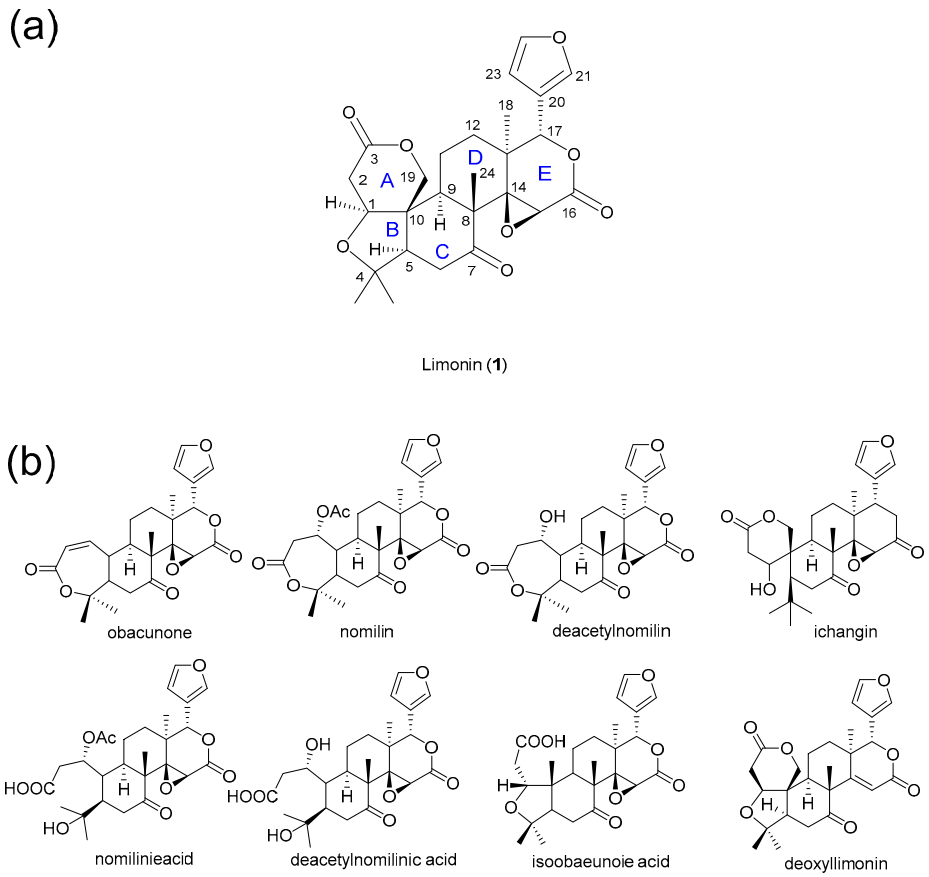


Figure 1. Structures of (**a**) limonin and (**b**) limonoids found in citrus fruits.

Limonoids, which are biosynthesized from euphane or tirucallane triterpenoids, can be divided into three categories, based on their chemical structures: limonoid aglycones, degraded limonoids, and limonoid glucosides. Among them, limonoid aglycones are the most abundant. Degraded limonoids are produced from limonoid aglycones by losing two rings, while limonoid glycosides are obtained by combining limonoid aglycones with glucose at the C-17 position via a glycosidic bond. Limonoid aglycones can be further categorized into the following five types according to their chemical structures and ring-opening forms: original form, A-ring opening, B-ring opening, C-ring opening, and A, D-rings-opening [4], of which the structures are shown in Figure 2.

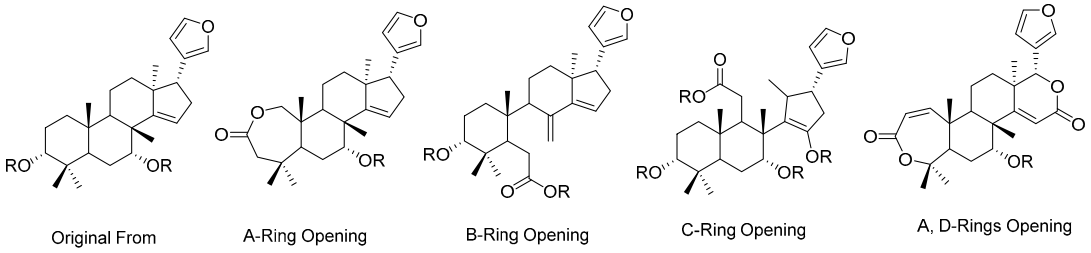


Figure 2. Several types of limonoid aglycones.

Since limonoids exhibit broad and remarkable biological activities, structurally modifying limonoids to improve the biological activities, as well as to understand the structure–

activity relationship, is promising. Due to the relatively rigid chemical structure of limonoids, there are only a few reports on the its structural modification, and these reports mainly focus on the carbonyl group at the 7 position. Giuseppe R. et al. carried out semisynthetic derivatization of limonoids and performed experimental studies on the antifeedant effect of beet armyworm larvae [d]. Among the derivatives, the compounds limonol, limonin-7-oxime, and limonin-7-methoxime showed significant antifeedant effects on beet armyworm larvae, with the antifeeding index of limonin-7-methoxime reaching 76%. Xu et al. made modifications at the C-7 position of limonin and synthesized a series of water-soluble limonin derivatives. They then studied the derivatives' biological activities regarding both anti-inflammatory and analgesic properties [4]. Among them, the biological anti-inflammatory activity of R_3 was better than that of the positive control drug, naproxen, and its analgesic effect was more evident than that of aspirin.

In this paper, the structure of limonin was modified through hydrogenation using different reductant agents, namely sodium cyanoborohydride, lithium aluminum hydride and sodium borohydride. A variety of reduction products were obtained and then characterized by a series of techniques, including High Resolution Electric Spray Ion Source Mass Spectrometry (HR-ESI-MS), Nuclear Magnetic Resonance (^{1}H-NMR, ^{13}C-NMR and 2D-NMR), and infrared spectrum (IR). The anti-inflammatory activities of the obtained limonin derivatives were then evaluated and compared with a series of natural limonins, using LPS-stimulated RAW264.7 cells and the BV2 cell model.

2. Materials and Methods

2.1. Materials

Limonin was purchased from the Sigma-Aldrich company. Other chemical reagents used in the structural modification of limonin were purchased from the Sinopharm Group. The details of reagents used in the cell experiments are provided in the supplementary information.

2.2. Hydrogenation of Limonin

2.2.1. Hydrogenation of Limonin Using Sodium Cyanoborohydride

First, 50 mg of limonin was dissolved in 5 mL of dichloromethane, and then 75 mg of sodium cyanoborohydride (dissolved in 1 mL of anhydrous methanol) was slowly added at 0 °C. Then, the solution was kept at room temperature for 8 h and then heated to 40 °C for another 4 h. During this period, thin layer chromatography (TLC) was employed to detect the products in the reaction system, which showed a new compound **2** was produced. Then, the dilute hydrochloric acid was added dropwise to quench the hydrogenation process, and adjusted to pH = 5, followed by extraction with dichloromethane (3 × 10 mL). The organic phase was dried over anhydrous sodium sulfate and concentrated under reduced pressure. The residue was isolated and purified using silica gel column chromatography (eluent using ethyl acetate: petroleum ether = 1:10) to obtain compound **2** (20 mg).

2.2.2. Hydrogenation of Limonin Using Lithium Aluminum Hydride

First, 100 mg of limonin was dissolved in 10 mL of anhydrous tetrahydrofuran (THF), and then 0.5 mL of 1 M lithium aluminum hydride tetrahydrofuran solution was added dropwise at 0 °C. After 1 h of reaction, TLC detected a new hydrogenation product **3**. The reaction system was quenched using the same procedure mentioned above. The solution was concentrated under reduced pressure to remove THF, and then water (15 mL) was added before extraction with ethyl acetate (20 mL × 3). The organic phase was dried over anhydrous sodium sulfate and concentrated under reduced pressure. The residue was isolated and purified by silica gel column chromatography (eluent using methanol:dichloromethane = 1:10) to obtain the main compound **3** (55 mg).

2.2.3. Hydrogenation of Limonin Using Sodium Borohydride

First, 150 mg of limonin was dissolved in 15 mL of dichloromethane, and then 70 mg of sodium borohydride (dissolved in 2 mL of anhydrous methanol) was added at 0 °C.

After 10 min of reaction, TLC detected that the raw materials were depleted in the solution, and a series of spots had formed, with the main spot having the same retention factor (R_f) as compound **2**. Therefore, 5 mL of the reaction solution was taken out and treated using the similar procedure mentioned above. The obtained compound was verified to be **2** (35 mg).

The remaining reaction solution was kept at 0 °C for 20 min. TLC detected two clearly product spots, and the content of compound **2** was significantly reduced. Therefore, 5 mL of the reaction solution was taken out and quenched. The solution was concentrated under reduced pressure to remove dichloromethane, and then water (10 mL) was added before extraction with ethyl acetate (15 mL × 3). The organic phase was dried over anhydrous sodium sulfate and then concentrated under reduced pressure. The residues were isolated and purified by silica gel column chromatography (eluent using ethyl acetate: petroleum ether = 1:10) to obtain compounds **4** (12 mg) and **5** (9 mg).

The remaining reaction solution was kept at 0 °C for another 90 min. TLC detected that compound **2** was completely consumed, and three new product spots merged. The pattern of the spots became complicated on the TLC plate. Thus, the reaction was quenched with dilute hydrochloric acid, adjusting to PH ≈ 5. The reaction solution was concentrated under reduced pressure to remove dichloromethane, and then water (10 mL) was added before extraction with ethyl acetate (15 mL × 3). The organic phase was dried over anhydrous sodium sulfate and concentrated under reduced pressure. The residues were isolated and purified by silica gel column chromatography (eluent using ethyl acetate: petroleum ether = 1:4) to obtain compounds **6** (8 mg), **7** (11 mg), and **8** (18 mg).

2.3. Evaluation of Anti-Inflammatory Activity

The mouse macrophage-like cell line RAW264.7 was used in the anti-inflammatory activity screening, obtained from the American Type Culture Collection (ATCC), Manassas, Virginia, USA. Mouse macrophages were cultured in a humidified incubator at 37 °C with a 5% CO_2 atmosphere. The basal medium was Dulbecco's Modified Eagle Medium (DMEM), containing 10% fetal bovine serum (FBS), 2 mmol/L glutamine, 100 μg/mL streptomycin, and 100 U/mL penicillin. An anti-inflammatory bioassay was performed using a similar procedure to that used by Xu et al. [17]. Generally, RAW264.7 cells and the compound with specific concentration (20 μM), or the control group, were incubated in the medium (0.125% dimethyl sulfoxide (DMSO)in the DMEM with 10% FBS). The cells were then stimulated with lipopolysaccharide (LPS, 1 μg/mL). After 24 h, the supernatant was obtained with centrifugation, and the inhibition ratio was determined using a TNF-α mouse ELISA kit. Dexamethasone was used as a positive control in the experiment.

In this study, the lipopolysaccharide (LPS)-induced murine microglial cells (BV2 cells) inflammation response model was used to further investigate the anti-inflammatory activity of the compounds. An amount of 100 ng/mL LPS was used to stimulate microglia in the experiment, releasing a large quantity of inflammatory factors, including NO. The content of NO in the supernatant was determined by the Griess test to preliminarily verify the inflammatory response of microglia. The specific steps of the experiment were as follows.

BV2 cells were, firstly, digested with 0.25% trypsin and suspended in DMEM, which contained high glucose and 10% FBS. They were then seeded on a 96-well plate at 2×10^5 cells/mL density, and the seeding volume was 100 μL/well. Next, the culture plate was placed in a 37 °C incubator containing 5% carbon dioxide. After the BV2 cells had been cultured for 24 h, the culture medium of each group was replaced with fresh DMEM, which was high in glucose and contained 10% FBS. The compounds (10 μL/well) were added to the dose-response group with a final concentration of 1 μM or 10 μM, and high-glucose DMEM with 10% FBS (10 μL/well) was added to the control group and the LPS model group. After 2 h of incubation, 0.001 mg/mL LPS (10 μL/well) was added to the dose-response group and the LPS model group, respectively, reaching a final concentration of 100 ng/mL. High-glucose DMEM, containing 10% FBS (10 μL/well), was added to the control group. After culturing for 24 h, 50 μL supernatant was taken from each well and 50 μL of Greiss

reagent was added to react at room temperature for 15 min. The optical density (OD) of each group was determined under a wavelength of 540 nm.

2.4. Cytotoxicity Evaluation

The cytotoxic effects of compounds on BV2 cells were determined by the following method. First, BV2 cells were dissociated with 0.25% trypsin and suspended in DMEM, which contained high glucose and 10% FBS. They were then seeded on a 96-well culture plate at 1.25 × 104 cells/mL, with a seeding volume of 100 µL/well. Next, the culture plate was placed in an incubator containing 5% CO_2 at 37 °C. After BV2 cells had been cultured for 24 h, the culture medium of each group was replaced with fresh DMEM, which was high in glucose and contains 10% FBS. The compounds (10 µL/well) were added to the dose-response group with a specific concentration of 1 µM or 10 µM, and high-glucose DMEM (10 µL/well) with 10% FBS was added to the control group. After culturing for another 24 h, 5 mg/mL MTT (10 µL/well) was added for live cell staining. After 3 h of incubation, the culture medium was discarded, and 100% DMSO (100 µL/well) was added, fully dissolving the cells on a plate shaker. The OD of each group was determined under a wavelength of 490 nm. An amount of 20 µL of resveratrol was used as a positive control in the experiment.

3. Results and Discussion

3.1. Hydrogenation of Limonin

Seven different hydrogenated limonin products (compounds **2**–**8**) were obtained using the various reagents. Through structural analysis, the reaction pathways of different reducing agents with limonin were determined.

Compound **2** was obtained by hydrogenation of limonin using sodium cyanoborohydride. It was a white amorphous powder, slightly soluble in dichloromethane and easily soluble in methanol. The NMR spectral data of compound 2 are shown in Figures S1 and S2. After data comparison with the literature [3], compound **2** was confirmed to be epi-limonol, a known compound. The structure of compound **2** and the reaction equation for the hydrogenation of limonin by sodium cyanoborohydride is illustrated in Figure 3. In summary, sodium cyanoborohydride only reduced the ketone carbonyl at the C-7 position to a secondary alcohol.

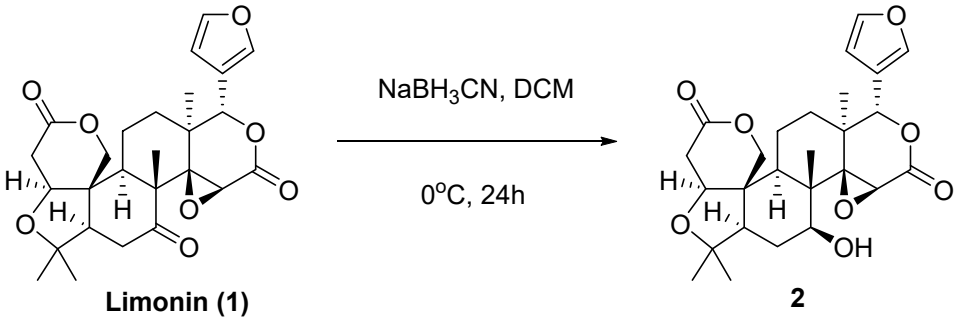


Figure 3. Hydrogenation of limonin by sodium cyanoborohydride.

Compound **3** was obtained by hydrogenating limonin with lithium aluminum hydride. It was also a white amorphous powder, which was not easily soluble in dichloromethane and easily soluble in methanol. According to HR-ESI-MS (Figure S3) {[M + Na]$^+$, *m/z* 505.2777, the calculated value was 505.2772} and the NMR spectra (Figures S4 and S5), its molecular formula could be inferred to be $C_{26}H_{42}O_8$, and the degree of unsaturation was six. Through the analysis of ^{13}C-NMR, Distortionless Enhancement by Polarization Transfer (DEPT), and Heteronuclear Single Quantum Coherence Spectroscopy (HSQC) spectra (Figure S6), it was confirmed that compound **3** had six quaternary carbons, eight methylene groups, eight methine groups, and four methyl groups. Combined analysis of HSQC and Heteronuclear Multiple Bond Correlation (HMBC) spectra (Figure S7) exhibited

the following: C-20 (δ_C 128.15), together with H-17 (δ_H 5.81) and H-18 (δ_H 1.07), had HMBC correlations; H-17, together with C-13 (δ_C 46.40), C-12 (δ_C 34.88), and C-14 (δ_C 86.55), together with C-18 (δ_C 17.22), had HMBC correlations; C-14, together with H-15 (δ_H 2.19) and C-16 (δ_H 3.62, 3.74), had HMBC correlations. Both C15 and C16 were methylene groups, indicating that the ternary epoxy was opened. During the opening of the ternary epoxy, the hydroxyl group attached at the C-14 position with the β configuration because the generated tertiary alcohol was more stable. The hydroxyl group of compound **3,** at the C-7 position, was examined with Nuclear Overhauser Effect Spectroscopy (NOESY) spectra (Figure S8). This showed that H-7 (δ_H 4.31), together with H-5 (δ_H 1.60) and H-9 (δ_H 1.53), were correlated with NOEs (Figure S9), confirming that the hydroxyl group at the C-7 position had the β configuration. The structure of **3** and the reaction equation of limonin hydrogenation by lithium aluminum hydride is illustrated in Figure 4. This reaction was a deep hydrogenation reaction, and **3** was in a highly reduced state.

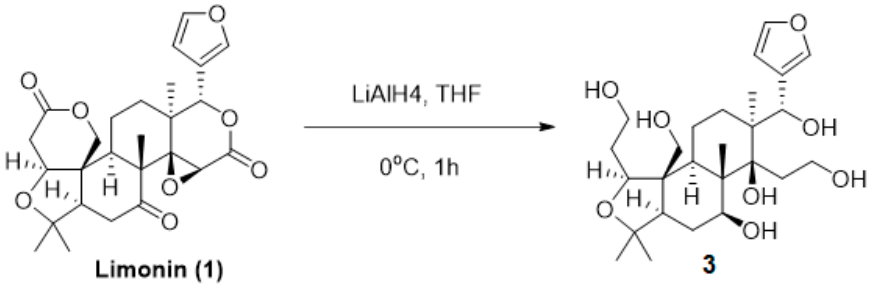


Figure 4. Hydrogenation of limonin by lithium aluminum hydride.

Compounds **4**–**8** were all white amorphous powders, which were not easily soluble in dichloromethane and easily soluble in methanol. They were produced in the reaction between limonin and sodium borohydride, with compound **2** as the intermediate product. Therefore, they were supposed to be the hydrogenation products of compound **2**.

The HR-ESI-MS characterization of compounds **4** and **5** showed the same *m/z* signal of 475.2336. According to the ^{1}H NMR and ^{13}C NMR data (Figures S10–S13), it could be inferred that they were isomers, having the same molecular formula as $C_{26}H_{34}O_8$, with the corresponding degree of unsaturation of 10. The IR (Figures S14 and S15) showed the signals of an ester carbonyl group (1733 cm^{-1}) and C=C bond (1680 and 960 cm^{-1}). From the ^{1}H-NMR data, it was observed that four methyl groups remained. Combined with the ^{13}C-NMR and DEPT spectral data, it was found that compounds **4** and **5** had one ester carbonyl group, five methylene groups, and seven quaternary carbons. Compared with compound **2**, one ester carbonyl group was lost in **4** and **5**. It could be inferred that the ester carbonyl group on ring A or ring B was reduced to a hydroxyl group. According to the 2D-NMR spectra of ^{1}H-^{1}H Correlated Spectroscopy (COSY) (Figures S16 and S17), HSQC (Figures S18 and S19), and HMBC (Figures S20 and S21), the carbonyl groups at the C-3 or C-16 position were also reduced. The configuration of these hydroxyl groups was then determined by the NOESY spectrum (Figures S22 and S23). First, C-20 (δ_C 124.83) correlated with H-17 (δ_H 4.97), confirming the hydrogen shifted on C-17 (δ_C 73.77). It was observed by the HMBC spectrum that H-17 was correlated with δ_C 38.38, δ_C 21.91, δ_C 68.65, and δ_C 89.07, respectively. In addition, δ_C 68.65 and δ_C 89.07 were attached to oxygen atoms, in which δ_C 68.65 was quaternary carbon, and δ_C 89.07 was methane. Thus, δ_C 68.65 was C-14, and δ_C 89.07 was C-16. According to ^{1}H-^{1}H COSY, H-15 (δ_H 3.96) correlated with H-16 (δ_H 5.30). Moreover, H-1 (δ_H 4.06) and H-19 (δ_H 4.46, 4.63) were correlated with C-3 (δ_C 173.73), respectively.

The relative configurations of compounds **4** and **5** were different. By analyzing their NOESY spectra (Figures S24 and S25) and the three-dimensional model, the relative configuration issues were primarily caused by the hydroxyl groups at C-7 and C-16 positions. Due to its rather rigid structure, limonin did not change the configuration at positions other than the reaction sites, such as H-1, H-4, H-9, and C-24. In the NOESY spectrum, H-5 (δ_H

1.99), H-7 (δ_H 3.94), and H-9 (δ_H 2.36) were correlated with each other, respectively; the methyl groups of H-16, H-15, and C-18 (δ_H 1.29) also showed NOE correlation with each other, respectively. Based on the above two groups of NOE correlations, both C-7 and C-16 positions of compound **4** were β-OH. The NOESY spectrum of compound **5** clearly showed the NOE correlation between H-7 and H-24 (δ_H 0.80), as well as the correlation between H-5 and H-9. In contrast, no NOE correlation with H-7 was seen. This proved that the C-7 position was α-OH, and also explained the difference in chemical shift around it. Furthermore, H-16 (δ_H 5.27), H-15 (δ_H 3.48), and H-18 (δ_H 1.28) also had NOE correlations with each other, respectively, confirming that compounds **5** and **4** were β-OH at C-16 position.

Compounds **6** and **7** were formed under the same conditions. They were obtained by the subsequent hydrogenation using sodium borohydride for 90 min on the basis of compounds **4** and **5**. The HR-ESI-MS results indicated that the two compounds shared the same *m/z* signal of 479.2644. Combined with the ^{1}H and ^{13}C NMR data (Figures S26–S29), it was deduced that they were isomers with the molecular formula of $C_{26}H_{38}O_8$, and the degree of unsaturation of eight. According to ^{13}C-NMR, DEPT, and HSQC spectra (Figures S30 and S31) analysis, compound **6** had six quaternary carbons, six methylene groups, 10 methine groups, and four methyl groups. Combined with the infrared spectrum analysis, no signal of ester carbonyl was observed. It was deduced that one of its rings was opened. From the perspective of structure stability, ring A and ring E, and the three-membered epoxy were more likely to be opened. By analyzing the HSQC and HMBC spectra (Figures S32 and S33), H-17 (δ_H 5.01) and C-16 (δ_C 89.10) had HMBC correlation, and C-15 (δ_C 59.2, δ_H, 3.40) was still methane. Therefore, the following findings were affirmed: the ring E and ternary epoxy were not opened; C-1 (δ_C 86.8) and H-2 (δ_H 1.91, 2.14)/H-3 (δ_H 3.64, 3.74) had HMBC correlation; C-10 (δ_C 51.90) and H-1 (δ_H 3.62)/H-19 (δ_H 3.96, 4.01) had HMBC correlation. Based on this, the ester bond of ring A was broken to form two primary alcohols. The above information confirmed the planar structures of compounds **6** and **7**.

Further efforts were paid to enclosing the configuration of the hydroxyl group at C-7 and C-16 positions, which might be the main difference between **6** and **7**. First, the comparison between the data of the ^{1}H and ^{13}C-NMR of compounds **5** and **6** showed that there was no noticeable difference. However, the NOESY spectrum (Figure S32) clearly showed NOE correlation between H-7 (δ_H 3.57) and H-24 (δ_H 1.09) and NOE correlation between H-16 (δ_H 5.30) and H-15/H-18 (δ_H 1.09), confirming that the hydroxyl group at the C-7 position of compound **6** was in α configuration, and the hydroxyl group at the C-16 position was in β configuration. Combined with the identification of isomer compounds **4** and **5**, the difference between compounds **7** and **6** in ^{1}H and ^{13}C data was essentially near the C-7 position. The assumption was that the hydroxyl group at the C-7 position was reversed, turning into β-OH.

The above assumption was confirmed by the NOESY spectrum (Figure S33) of compound **7**, which showed that H-7 (δ_H 4.02), H-5 (δ_H 1.70), and H-9 (δ_H 2.09) had NOE correlation, and H-16 (δ_H 4.93), together with H-15 (δ_H 3.83) and H-18 (δ_H 1.29), had NOE correlation, confirming that compound **7** was β-OH at both C-7 and C-16 positions.

Compound **8** was shown to be relatively more polar when detected in TLC. According to HR-ESI-MS {$[M + H]^+$, *m/z* 481.2806, the calculated value was 481.2796} and, with the NMR spectra ^{1}H and ^{13}C data (Figures S34 and S35), it was deduced that its molecular formula was $C_{26}H_{40}O_8$, and its degree of unsaturation was seven. According to the analysis of ^{13}C-NMR, DEPT, and HSQC spectra (Figure S36), compound **8** had six quaternary carbons, seven methylene groups, nine methine groups, and four methyl groups. In the infrared spectrum, no signal of ester carbonyl was observed either. Combined analysis of HSQC and HMBC spectra (Figure S37) showed the following: C-20 (δ_C 127.70), together with H-17 (δ_H 4.96) and H-18 (δ_H 1.30), had HMBC correlation; H-17, together with C-13 (δ_C 44.20), C-12 (δ_C 30.80), C-14 (δ_C 78.50), and C-18 (δ_C 23.81), had HMBC correlation; C-14, together with H-15 (δ_H 3.80) and C-16 (δ_H 3.76, 4.02), had HMBC correlation. C-16 was methylene, which meant that ring E was opened and the ester bond was reduced to two

primary alcohols. Referring to compounds **6** and **7**, ring A was also opened. The only site where compound **8** had a configuration issue was the hydroxyl group at the C-7 position. The NOESY spectrum (Figure S38) clearly showed the NOE correlation between H-7 (δ_H 3.57) and H-24 (δ_H 1.09); H -16 (δ_H 5.30) and H-15/H-18 (δ_H 1.09) had NOE correlation. It was confirmed that, for compound **6**, the hydroxyl group at the C-7 position was in α configuration, and the hydroxyl group at the C-16 position was in β configuration.

The structural identification of the above products showed that the hydrogenation of limonin using sodium borohydride was more complicated than that when using sodium cyanoborohydride. The structures of the above products are summarized in Figure 5. Among them, compound **2** was the preliminary hydrogenation product; compounds **4** and **5** were isomers, which were the products of further hydrogenation of compound **2**; compounds **6** and **7** were isomers, which were the products of further hydrogenation of compounds **4** and **5**; compound **8** was the deep hydrogenation product.

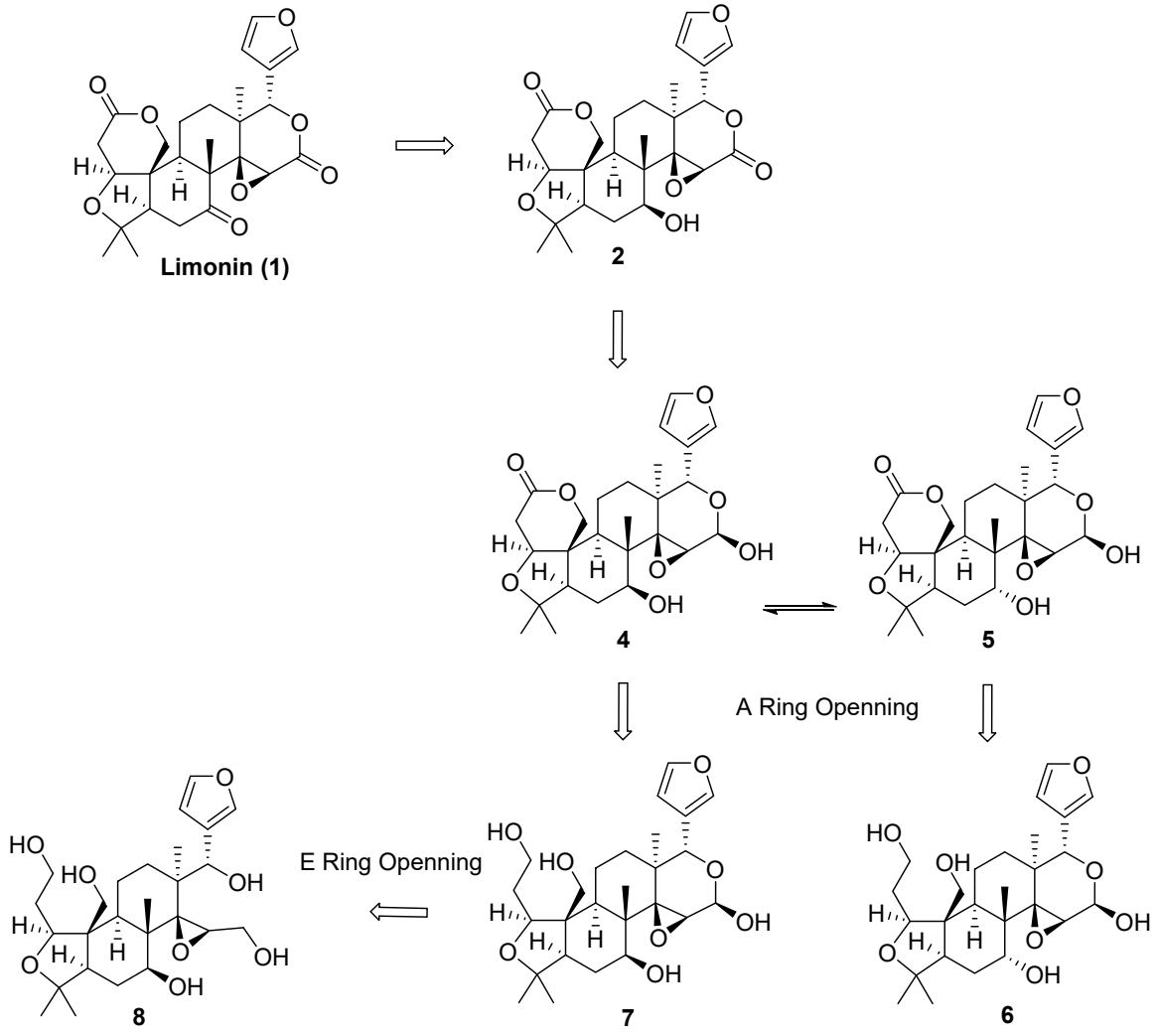


Figure 5. Hydrogenation of limonin by sodium borohydride.

The above results suggested a reagent-dependent hydrogenation mechanism for limonoid. When using the mild reducing agent of sodium cyanoborohydride, only the preliminary hydrogenation product was obtained. In comparison, when using a stronger reducing agent, such as sodium borohydride, various limonoid derivatives could be obtained with different degrees of reduction according to the duration of the reactions. This suggested that sodium cyanoborohydride reacted more gently than sodium borohydride and had better product selectivity. However, lithium aluminum hydride, which has strong

reducing capability, offered an intensive reaction. Thus, only highly reduced limonoid derivatives could be obtained.

3.2. Evaluation of Anti-Inflammatory Activity of Limonoids

The anti-inflammatory activity of the seven obtained limonoid derivatives, together with another eight natural limonoid compounds [18], shown in Figure 6, was evaluated and compared with the use of cell experiments.

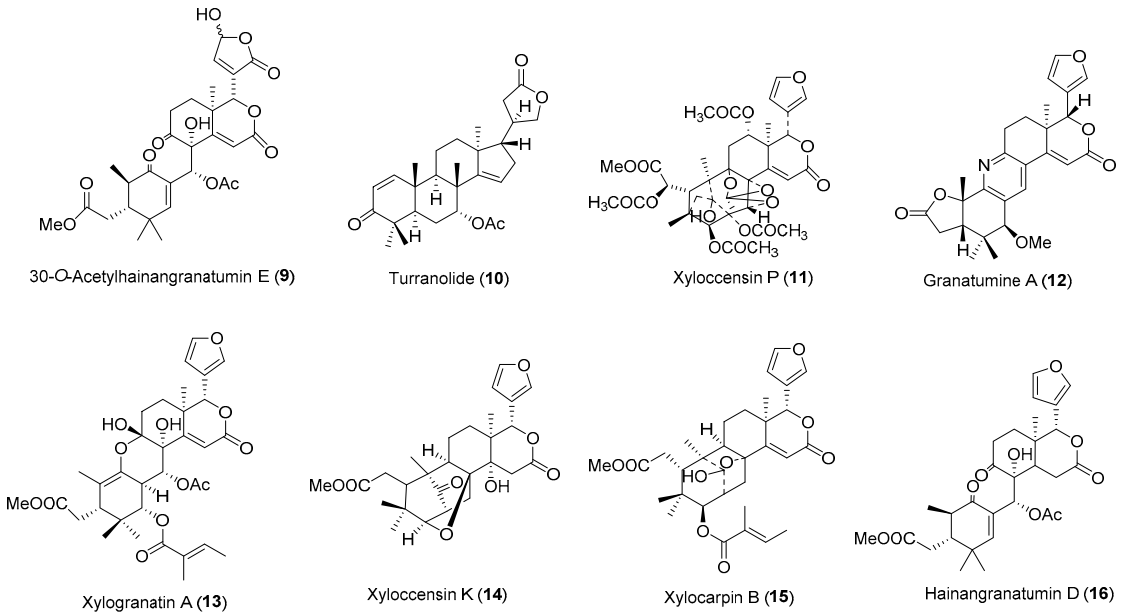


Figure 6. Eight Natural Limonoid Compounds Studied in This Work.

The results of the anti-inflammatory activity bioassay of mouse macrophage cells RAW264.7 are listed in Table 1. The natural compounds 30-O-Acetylhainangranatumin E (**9**) and Xylgranatin A (**13**) obviously inhibited LPS-induced RAW264.7 cells from producing and releasing inflammatory factors, such as TNF-α. Compound **13** was particularly prominent, of which the inhibition ratio reached 90.0%. The inhibition ratio of compound **9** was 55.3%. Other natural limonoid derivatives possessed a relatively low inhibition ratio, especially for compounds **11**, **12**, and **15**, which did not show any inhibitory effects. This result was consistent with the results of Chen's work, in which the studied natural limonoid derivatives also showed vastly different inhibition ratios, ranging from 10.5 to nearly 100%, at the same concentration of 20 μM [19]. In contrast, the seven compounds yielded by the hydrogenation of limonin all showed decent anti-inflammatory activity. Their inhibition ratio of TNF-α, an inflammatory factor released by LPS-induced RAW264.7 cells, ranged from 26.9 to 37.8%. Among them, compound **3**, which had a high degree of hydrogenation, presented the highest inhibition ratio of 37.8%, while compound **2**, which was only slightly hydrogenated, presented the lowest inhibition ratio of 26.9%. The result suggested that the anti-inflammatory activities of hydrogenation products of limonin were related to the degree of hydrogenation.

Table 1. Experiment results of anti-inflammatory activity screening of limonoids.

Compound (#)	Concentration μM	Mean Release of TNF-α by RAW264.7 Cells (pg/mL)	SD Value	Inhibition Ratio of TNF-α Release (%)
	Cell Control	**70.5**	**9.0**	
	Stimulation Control	**3602.5**	**461.1**	
2	20	2592.3	140.1	28.6 *
3	20	2266.4	172.6	37.8 ***
4	20	2506.6	59.8	31.0 ***
5	20	2504.3	152.2	30.5 **
6	20	2501.6	155.0	31.2 **
7	20	2398.1	161.0	33.4 **
8	20	2432.7	147.2	32.5 *
9	20	1956.1	174.6	55.3 ***
10	20	3379.4	173.8	18.0
11	20	4395.4	290.9	−8.6
12	20	4179.9	478.5	−3.0
13	20	636.3	127.1	90.0 ***
14	20	3416.5	834.2	17.0
15	20	4686.7	489.3	−16.3
16	20	2770.8	287.4	34.0 **

Significance: * $p < 0.05$; ** $p < 0.01$; *** $p < 0.001$ vs. LPS control. N = 4.

Moreover, the BV2 cell model was employed to further investigate the ameliorating effects and cytotoxicity of limonoid compounds on LPS-induced BV2 cell inflammation. The results are shown in Table 2. The natural limonoid derivatives **9**, **10**, **13**, **14**, and **16** presented inhibitory ratios of NO greater than 30% on LPS-induced BV2 cell inflammation at a concentration of 10 μM. Among them, compound **13** had the best inhibitory activity on LPS-induced BV2 cell inflammation, corresponding to an inhibitory ratio of 63.77%. The better bioactivity of **13** might be related to the unique 2,3-dimethacrylate group. Similar results were observed in An's study, which showed that natural limonoid derivatives with 2,3-dimethacrylate group generally presented higher anti-inflammatory activity [20]. Among the seven compounds obtained by the hydrogenation of limonin, compound **3** offered the best result at 1 μM concentration, and the inhibitory ratio of NO was 10.27%, which was comparable to that of natural derivatives **9**, **15**, and **16**. At 10 μM concentration, compound **8** gave the best result of a 16.16% NO inhibitory ratio.

In addition to anti-inflammation activity, the cytotoxicity of limonoid derivatives were also evaluated (Table 3). At the concentration of 1 μM, all compounds discussed in this study showed low cytotoxicity, with cell viability in the range of 93–100%. However, at the concentration of 10 μM, compound **11** showed slightly more cytotoxicity with a cell viability of 88.1%. Compared to natural limonoid derivatives, the seven synthesized limonoid derivatives were less cytotoxic, and the corresponding cell viabilities were all higher than 90% at 10 μM. The better safety and gentleness of the synthesized compounds should be ascribed to the very low cytotoxicity of limonin, which has been widely demonstrated in BV2 cells and other cell models [21,22].

Table 2. The ameliorating effects of compounds on LPS-induced BV2 cell inflammation.

Groups	NO Production ± SEM (% of LPS Group)			
Control	3.35% ± 1.54			
Model-LPS (100 ng/mL)	100.0% ± 0.00			
Positive control-Resveratrol (20 μM)	70.64% ± 0.98 ***			
Compounds	**1 μM**	**Inhibition Ratio of NO**	**10 μM**	**Inhibition Ratio of NO**
2	97.94% ± 6.92	2.06%	87.40% ± 9.08	12.60% *
3	89.73% ± 4.66	10.27%	88.44% ± 2.32 *	11.56% **
4	105.3% ± 5.69	−5.30%	86.57% ± 6.21	13.43% *
5	108.6% ± 6.83	−8.60%	100.7% ± 2.37	−0.70%
6	101.2% ± 5.42	−1.20%	88.43% ± 3.31	11.57% **
7	93.23% ± 6.16	6.77%	100.6% ± 9.64	−0.60%
8	98.66% ± 8.01	1.34%	83.84% ± 2.12	16.16%
9	87.35% ± 7.08	12.65%	63.48% ± 7.67	36.52% ***
10	103.3% ± 8.02	−3.30%	54.37% ± 7.30	45.63% **
11	90.78% ± 4.67	9.22%	83.33% ± 2.68	16.67% **
12	96.51% ± 5.01	3.49%	85.10% ± 3.98	14.90% **
13	91.37% ± 3.43	8.63%	36.23% ± 2.93	63.77% ***
14	95.47% ± 8.39	4.53%	64.16% ± 1.56	35.84% ***
15	88.40% ± 4.38	11.60%	81.61% ± 2.55	18.39% **
16	89.86% ± 3.79	10.14%	67.60% ± 2.33	32.40% ***

Significance: * $p < 0.05$; ** $p < 0.01$; *** $p < 0.001$ vs. LPS control. N = 4.

Table 3. Cytotoxicity of compounds on BV2 Cells.

Groups	Cell Viability ± SEM (% of the Control Group)	
Control	100.0% ± 0.00	
Positive control-Resveratrol (20 μM)	57.72% ± 3.21	
Compounds	**1 μM**	**10 μM**
2	99.64% ± 4.13	95.65% ± 3.70
3	93.14% ± 3.77	95.11% ± 3.80
4	94.96% ± 2.83	92.97% ± 1.97
5	104.0% ± 4.67	101.2% ± 1.69
6	101.4% ± 5.23	91.67% ± 0.69
7	96.55% ± 3.49	90.20% ± 3.85
8	98.56% ± 2.51	91.97% ± 1.14
9	100.4% ± 3.99	92.44% ± 3.12
10	102.4% ± 1.65	92.73% ± 2.92
11	101.5% ± 2.37	88.10% ± 3.68
12	99.00% ± 1.88	91.42% ± 1.46
13	101.5% ± 0.90	90.74% ± 2.47
14	99.45% ± 2.69	96.86% ± 4.92
15	96.98% ± 4.55	97.10% ± 1.06
16	97.80% ± 4.53	97.63% ± 2.78

4. Conclusions

The hydrogenation of limonin, with a variety of reducing agents, was investigated in this paper. Seven hydrogenation products, of which six were unreported new compounds in the literature, were obtained. The planar structures and spatial configurations were identified using HR-ESI-MS, 1D-NMR (^{1}H and ^{13}C), 2D-NMR, and IR analysis. The six hydrogenated limonoid products were evaluated and compared with eight natural limonoid compounds. The study found that the hydrogenated products all showed decent anti-inflammatory activity. Among them, compound **3** had the highest inhibitory ratio on the inflammatory factor TNF-α released by LPS-induced RAW264.7 cell, reaching 37.8%.

Among the natural limonoids, compound **13** had the highest inhibition ratio of inflammatory factors, reaching 90%. At a concentration of 10 μM, among the natural limonoids, compound **13** had the best inhibitory activity on LPS-induced BV2 cell inflammation, with a NO inhibition ratio of 63.77%. However, the inhibition ratios of synthesized limonoid derivatives were generally lower than those of the natural limonoids.

The natural limonoid compound Xylgranatin A (**13**) was verified to have outstanding anti-inflammatory activity in the two LPS-induced inflammation models. Among the limonoids synthesized through hydrogenation in this paper, the anti-inflammatory activity of compound **3** was more prominent, and it was superior to most natural limonoid derivatives in the evaluation of RAW264.7 cells.

Supplementary Materials: The following supporting information can be downloaded at: https://www.mdpi.com/article/10.3390/app122111169/s1.

Author Contributions: Conceptualization, J.Y. and Y.H.; methodology, J.Y. and Y.H.; formal analysis, J.Y.; investigation, K.C.; resources, Y.H.; data curation, J.Y.; writing—original draft preparation, K.C.; writing—review and editing, K.C. All authors have read and agreed to the published version of the manuscript.

Funding: This research received no external funding.

Conflicts of Interest: The authors declare no conflict of interest.

References

1. Yong, W.T. Advances in pharmacological activities of limonoid monomers. *Chin. Med. Mater.* **2017**, *40*, 242–246.
2. Jiang, J.P. A review: Research progress of limonoids. *China Brew.* **2012**, *31*, 10–14.
3. Ruberto, G.; Renda, A.; Tringali, C.; Napoli, E.M.; Simmonds, M.S.J. *Citrus* limonoids and their semisynthetic derivatives as antifeedant agents against *Spodoptera frugiperda* larvae. a structure-activity relationship study. *J. Agric. Food Chem.* **2002**, *50*, 6766–6774. [CrossRef]
4. Yang, Y.; Wang, X.; Zhu, Q.; Gong, G.; Luo, D.; Jiang, A.; Yang, L.; Xu, Y. Synthesis and pharmacological evaluation of novel limonin derivatives as anti-inflammatory and analgesic agents with high water solubility. *Bioorg. Med. Chem. Lett.* **2014**, *24*, 1851–1855. [CrossRef]
5. Fan, S.M.; Zhang, C.L.; Luo, T. Limonin: A review of its pharmacology, toxicity, and pharmacokinetics. *Molecules* **2019**, *24*, 3679. [CrossRef]
6. Kim, W.; Fan, Y.-Y.; Smith, R.; Patil, B.; Jayaprakasha, G.K.; McMurray, D.N.; Chapkin, R.S. Dietary curcumin and limonin suppress $CD4^+$T-cell proliferation and interleukin-2 production in mice. *J. Nutr.* **2009**, *139*, 1042–1048. [CrossRef]
7. Kim, J.; Jayaprakasha, G.K.; Muthuchamy, M.; Patil, B.S. Structure–function relationships of citrus limonoids on p38 MAP kinase activity in human aortic smooth muscle cells. *Eur. J. Pharmacol.* **2011**, *670*, 44–49. [CrossRef]
8. Hassan, N.A.; Bassossy, H.M.E.; Fahmy, A.; Mahmoud, M.F. Limonin alleviates macro- and micro-vascular complications of metabolic syndrome in rats: A comparative study with azelnidipine. *Phytomedicine* **2018**, *43*, 92–102. [CrossRef]
9. Fujii, A.; Okuyama, T.; Wakame, K. Identification of anti-inflammatory constituents in Phellodendri Cortex and Coptidis Rhizoma by monitoring the suppression of nitric oxide production. *J. Nat. Med.* **2017**, *71*, 745–756. [CrossRef]
10. Wang, Y.J.; Lu, Y.; Zhou, Y.F.; Wang, Y.; Guo, S.H.; Zhang, Q.; Sun, Y. Therapeutic effect and mechanism of limonin on dextran sulfate sodium salt-induced ulcerative colitis in mice. *Chin. J. Biopr. Eng.* **2018**, *16*, 57–62.
11. Wang, D.; Zhang, H.H.; Fang, J.; Zhong, Y.; Yu, C. Effects of limoninon on LPS-induced acute lung injury in mice. *Chin. J. Clinc. Pharmacol. Therapeut.* **2018**, *23*, 8–12.
12. Liu, M.H.; Zhou, X.D. Limonin inhibits the PM2.5 inhalation-induced airway inflammation and mucus hypersecretion in rats. *Basic Med. Sci. Clin.* **2018**, *38*, 433–438.
13. Wang, X.; Zhou, Y.; He, S.; Ouyang, Z.; Feng, L.; Shen, Y.; Wu, X.; Sun, Y.; Wu, X.; Xu, Q. Obaculactone exerts a novel ameliorating effect on contact dermatitis through regulating T lymphocyte. *Int. Immunopharmacol.* **2015**, *28*, 1–9. [CrossRef]
14. Zhang, A.; Wang, H.; Sun, H.; Zhang, Y.; An, N.; Yan, G.; Meng, X.; Wang, X. Metabolomics strategy reveals therapeutical assessment of limonin on nonbacterial prostatitis. *Food Funct.* **2015**, *6*, 3540–3549. [CrossRef]
15. Langeswaran, K.; Revathy, R.; Vijayaprakash, S.; Balasubramanian, M.; Gowthamkumar, S. Influence of limonin on Wnt signalling molecule in HepG2 cell lines. *J. Nat. Sci. Biol. Med.* **2013**, *4*, 126–133. [CrossRef]
16. Langeswaran, K.; Jagadeesan, A.J.; Revathy, R.; Balasubramanian, M.P. Chemotherapeutic efficacy of limonin against Aflatoxin B1 induced primary hepatocarcinogenesis in Wistar albino rats. *Biomed. Aging Pathol.* **2012**, *2*, 206–211. [CrossRef]
17. Xu, R.; Ma, L.; Chen, T.; Wang, J. Sophorolipid Suppresses LPS-Induced Inflammation in RAW264. 7 Cells through the NF-κB Signaling Pathway. *Molecules* **2022**, *27*, 5037. [CrossRef]

18. Zhou, Z.; Kurtán, T.; Mándi, A.; Gu, Y.; Yao, L.; Xin, G.; Li, X.; Guo, Y. Novel and neuroprotective tetranortriterpenoids from Chinese mangrove Xylocarpus granatum Koenig. *Sci. Rep.* **2016**, *6*, 33908. [CrossRef]
19. Chen, Y.; Ruan, J.; Sun, F.; Wang, H.; Yang, S.; Zhang, Y.; Yan, J.; Yu, H.; Guo, Y.; Zhang, Y.; et al. Anti-inflammatory limonoids from Cortex Dictamni. *Front. Chem.* **2020**, *8*, 73. [CrossRef]
20. An, F.; Wang, X.; Yang, M.; Luo, J.; Kong, L. Bioactive A-ring rearranged limonoids from the root barks of Walsura robusta. *Acta Pharm. Sin. B* **2019**, *9*, 545–556. [CrossRef]
21. Liu, Z.; Lu, S.; Zhang, J.; Chen, X.; Mickymaray, S. Limonin: A triterpenoid exerts protective effect during lipopolysaccharide stimulated inflammation in BV2 microglial cells. *Pharmacogn. Mag.* **2020**, *16*, 859. [CrossRef]
22. Liu, S.; Zhang, S.; Lv, X.; Lu, J.; Ren, C.; Zeng, Z.; Zheng, L.; Zhou, X.; Fu, H.; Zhou, D.; et al. Limonin ameliorates ulcerative colitis by regulating STAT3/miR-214 signaling pathway. *Int. Immunopharmacol.* **2019**, *75*, 105768. [CrossRef]